Aerospace Science and Technology 48 (2016) 115–121

Contents lists available at ScienceDirect

Aerospace Science and Technology

www.elsevier.com/locate/aescte

Short communication

Effect of a pusher propeller on a delta wing

L.W. Traub

Aerospace and Mechanical Engineering Department, Embry Riddle Aeronautical University, Prescott, USA

ARTICLE INFO

Article history:
Received 12 October 2015
Received in revised form 10 November 2015
Accepted 13 November 2015
Available online 17 November 2015

ABSTRACT

A low speed wind tunnel investigation was conducted to examine the effect of a pusher propeller on a 65 deg sweep delta wing. Two different propeller diameters were evaluated. The data showed that the pusher geometry can cause a delay in vortex breakdown yielding an increase in lift at high angles of attack. Surface pressure measurement showed that the propeller increased suction levels on both the leeward and windward surfaces, limiting lift enhancement. Lift augmentation was observed to favor low advance ratios.

1. Introduction

Widespread application and use of small unmanned aerial vehicles (UAVs) has resulted in an ongoing and sustained research effort to enhance their efficiency. The low Reynolds number environment of operation of these vehicles has yielded planform solutions that are generally of low aspect ratio. Studies by Torres and Mueller [1] as well as Chen and Qin [2] have indicated that planforms such as the Zimmerman, are effective. Issues encountered by these flight vehicles include low Re effects (laminar separation and bubbles) and susceptibility to atmospheric turbulence. A candidate wing form for a small UAV with characteristics that are well documented is the delta wing. It has low sensitivity to Re [3] and due to its low lift curve slope, atmospheric turbulence. Its geometry also promotes structural rigidity and weight effectiveness.

Thin sharp edged delta wings are characterized by the formation of conical leading edge vortices [4,5]. These vortices enhance lift due to induced suction and are inherently inviscid in nature (as numerical solution using Euler solvers indicates). As wing sweep increases, the leading edge vortex strength decreases; however the vortex lift constitutes an increasing proportion of the total lift. At high incidence the leading edge vortices experience vortex breakdown (VBD) [5–8]. Vortex bursting is associated with a stagnation of the axial velocity along the vortex core and a disruption of the organized spiral structure of the vortices ultimately causing a breakdown to turbulence. Breakdown deleteriously affects lift and pitching moment. Increasing sweep increases the impact of breakdown on lift but delays the initial onset of vortex breakdown [8]. As shown in Ref. [9], small UAVs often have delta geometries that are not considered slender, i.e. the leading edge sweep angle is 55 deg or less. For these wings, Reynolds number sensitivity may be apparent because the leading edge vortices form close to the surface such that viscous interactions become important.

An adverse pressure gradient and a high swirl angle are causative in the onset and progression of breakdown. Consequently, enforcement of the Kutta condition at the wing's trailing edge serves as an initiator of VBD. Studies have shown that the use of a trailing edge jet can successfully delay the onset of VBD [10–16]. Jet blowing at the trailing edge delays VBD by modifying the axial pressure gradient. Trailing edge blowing is sweep dependent with increasing sweep enhancing effectiveness. However, for a small UAV, such an application is not feasible. Most small UAVs are propeller powered. Consequently, it is of interest to examine the impact of a propeller in a pusher configuration on the aerodynamics of a delta wing. The induced propeller flow may serve to modulate the wing's trailing edge pressure field and thus VBD. This article presents an examination of such a configuration using both force balance and surface pressure measurement.

2. Equipment and procedure

Wind tunnel testing was undertaken in Embry Riddle University's 0.812 m by 1.143 m wind tunnel. This tunnel has a turbulence intensity of approximately 0.3% for the range of test velocities. Force and moment acquisition was facilitated using an Aerolab 6-component Pyramidal balance. Prior to use, the balance calibration was checked through the application of known loads. Load accuracy has been established as 0.098 N for lift. Angle of attack (α) can be set within 0.02 deg. All displayed data points represent the average of 1000 readings. Testing was undertaken at veloci-

E-mail address: traubl@erau.edu.

http://dx.doi.org/10.1016/j.ast.2015.11.010
1270-9638/

Pressure Tap Locations

2y/s (x/c_{root}=0.81)	2y/s (x/c_{root}=0.93)
0.12	0.15
0.20	0.24
0.28	0.31
0.35	0.40
0.43	0.48
0.50	0.55
0.58	0.60
0.66	0.63
0.69	0.67
0.74	0.72
0.77	0.76
0.81	0.80
0.84	0.83
0.88	0.88
0.96	0.95

y = spanwise co-ordinate
s = local semi-span

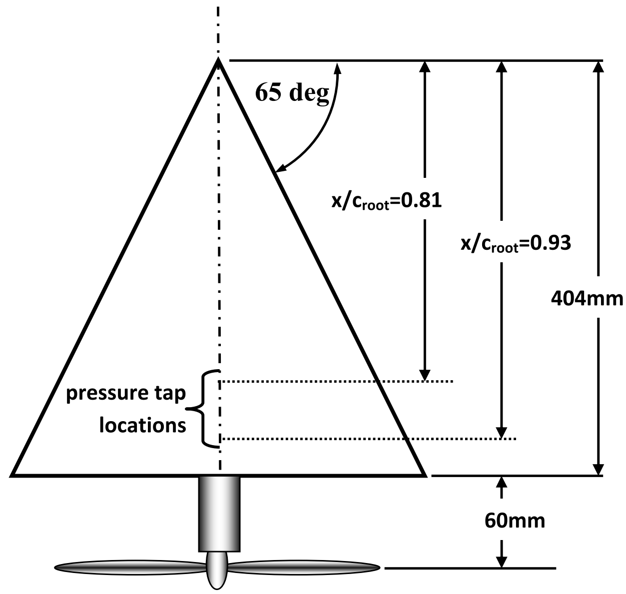

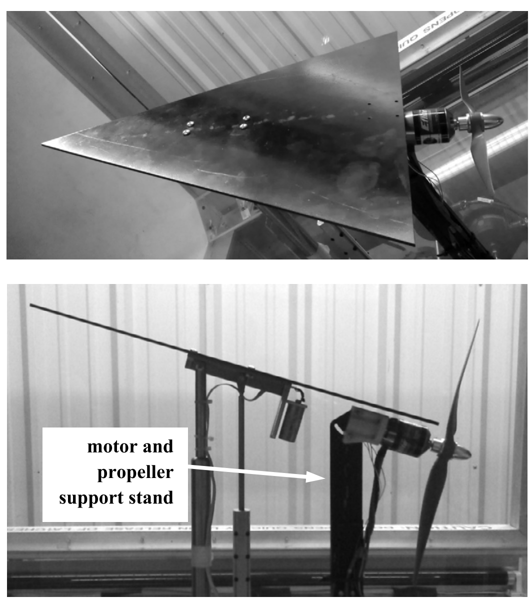

Fig. 1. Model geometry an images of installation.

ties (U) of 10, 15 and 20 m/s yielding Re = 150,000, 225,000 and 300,000 respectively, based on the mean aerodynamic chord length of 0.27 m. Due to the comparative nature of the testing, wall corrections where not employed.

Two 65 deg leading edge sweep delta wings were fabricated from 3.18 mm thick steel plate; one for force balance use and the other for surface pressure measurement. Due to the low thickness to chord ratio, the wing leading edges where not beveled. The root chord was 0.404 m. The moment reference length was that of the mean aerodynamic chord (2/3 of the root chord, c_{root}). Moments were taken about the mid-root chord location. Twelve (0.305 m) (APC 12-6P) and eight (0.203 m) (APC 8-6P) inch diameter Advance Precision Composites (APC) two bladed propellers were evaluated. The propellers where attached to an E-flite brushless outrunner motor which was in turn governed using a servo controller in conjunction with an E-flite electronic speed controller. Power was supplied using a lawnmower battery. The propellers extended to 80% and 54% of the trailing edge span. To clearly extract the aerodynamic forces and avoid contamination by propeller thrust required that the propeller–motor was mounted separately from the wing. Consequently, a bracket was fabricated that allowed setting of the propulser and adjustment for wing incidence, see Fig. 1. The bracket was attached to the wind tunnel floor. Propeller frequency (f) was monitored using an Optek infrared phototransistor with an output signal read using a Fluke 175 multi-meter. Propeller rotation rate could be set and maintained within 0.2 Hz. Geometrical constraints yielded a propeller hub installation 22 mm below the wing and 60 mm aft of the trailing edge.

The pressure tapped model contained two rows of tappings as indicated in Fig. 1. Small bore Tygon tubing (0.79 mm internal diameter) was used to connect the ports to an electronic pressure scanner. The scanner contains thirty independent pressure transducers and can be scanned at upto 250,000 readings per second. Accuracy has been established as better than 1 Pa.